Transient Receptor Potential (TRP) Channels and Calcium Signaling

Laura Vangeel and Thomas Voets

Laboratory of Ion Channel Research, VIB Center for Brain & Disease Research, Department of Cellular and Molecular Medicine, University of Leuven, Leuven, Belgium

*Corresponding authors: Laura.Vangeel@kuleuven.vib.be; Thomas.Voets@kuleuven.vib.be

1. Abstract

Transient Receptor Potential (TRP) cation channels play diverse roles in cellular Ca^{2+} signaling. First, as Ca^{2+}-permeable channels that respond to a variety of stimuli, TRP channels can directly initiate cellular Ca^{2+} signals. Second, as non-selective cation channels, TRP channel activation leads to membrane depolarization, influencing Ca^{2+} influx via voltage-gated and store-operated Ca^{2+} channels. Finally, Ca^{2+} modulates the activity of most TRP channels, allowing them to function as molecular effectors downstream of intracellular Ca^{2+} signals. Whereas the TRP channel field has long been devoid of detailed channel structures, recent advances, particularly in cryo-electron microscopy-based structural approaches, have yielded a flurry of TRP channel structures, including members from all seven subfamilies. These structures, in conjunction with mutagenesis-based functional approaches, provided important new insights into the mechanisms whereby TRP channels permeate and sense Ca^{2+}. These insights will be highly instrumental in the rational design of novel treatments for the multitude of TRP channel-related diseases.

2. Introduction to TRP channels and Ca^{2+} signaling

TRP channels form a large branch within the superfamily of voltage-gated cation channels, which further contains the K^+-selective channels, voltage-gated Na^+ channels, voltage-gated Ca^{2+} channels, cyclic nucleotide-gated channels and two pore (TPC channels) (Yu and Catterall 2004). The human genome encodes 27 TRP channel-encoding genes (Gees et al. 2012), and further TRP channel-encoding genes are found in all vertebrates, insects, worms, yeast and even single-celled algae (Harteneck et al. 2000; Arias-Darraz et al. 2015). The designation TRP originates from the *trp* gene in *Drosophila*, disruption of which leads to a *t*ransient *r*eceptor *p*otential in the fly photoreceptors (Minke et al. 1975). As such, the name TRP is a relic from the past rather than an accurate description of the physiological properties of this family of channels, which are involved in diverse biological and pathophysiological processes, mostly completely unrelated to the transient nature of receptor potentials (Clapham 2003; Nilius et al. 2007; Venkatachalam and Montell 2007; Gees et al. 2012).

However, finding a more apt name for this group of channels is not evident: the TRP channel family is really a mixed bag, consisting of cation channels exhibiting a wide range of ion selectivities, gating mechanisms and biological functions. Arguably, the most common feature of TRP channels is that they make a substantial impact on cellular Ca^{2+} signaling. In particular, TRP channels can act as pathway for Ca^{2+} to enter the cytosol, modulate the activity of other Ca^{2+}-permeable channels, and translate changes in cytosolic Ca^{2+} into cation flux and electrical activity.

In this review, we summarize and discuss recent insights into the role of TRP channels in cellular Ca^{2+} signaling, with particular focus on the structural determinants of TRP channel- Ca^{2+} interactions.

3. Ca^{2+} action and reaction

Ca^{2+} is a ubiquitous intracellular messenger, and Ca^{2+} signaling lies at the basis of innumerous biological processes, including cell adaptation, survival and cell death (Berridge 2017). Adequate spatiotemporal regulation of intracellular Ca^{2+} therefore represents a central theme in every cell. TRP channels are tightly involved both in shaping Ca^{2+} signals and in responding to physiological changes in intracellular Ca^{2+} in animal cells.

TRP channel gating shaping cytosolic Ca^{2+} signals

Based upon their relative permeability to Ca^{2+} and Na^{+} (P_{Ca}/P_{Na}), TRP channels can roughly be divided into three groups (Owsianik et al. 2006) (Fig. 1). The majority of TRP channels are Ca^{2+}-permeable non-selective cation channels with P_{Ca}/P_{Na} values in the range between 0.1 and 20. In most cell types, opening of these TRP channels will induce an inward current that is carried by a mixture of Na^{+} and Ca^{2+} ions (Mulier et al. 2017). The two closely homologous epithelial TRP channels TRPV5 and TRPV6 are exquisitely Ca^{2+}-selective, with estimated P_{Ca}/P_{Na} values exceeding 100 (Vennekens et al. 2000; Yue et al. 2001). Under physiological ionic conditions, these channels will generate inward currents that are almost exclusively carried by Ca^{2+} ions, similar to the high Ca^{2+} selectivity of voltage-gated Ca^{2+} channels and store-operated Orai1 channels. TRPM4 and TRPM5 are situated on the other end of the selectivity spectrum, showing negligible permeability to Ca^{2+} ions ($P_{Ca}/P_{Na} < 0.01$). Inward currents mediated by these channels are mainly carried by Na^{+} ions (Launay et al. 2002; Prawitt et al. 2003; Nilius et al. 2005).

Notwithstanding this diversity in the ion selectivity of their pores, it has already been well-established in the pre-structural-era that TRP channels share a common overall architecture, analogous to that of voltage-gated channels that mediate K^{+}, Na^{+} or Ca^{2+} flux (Gaudet 2008). All TRP channel family members are proteins containing six transmembrane domains (S1 to S6) and relatively long intracellular N- and C-termini. After assembly of four such TRP subunits into one functional tetramer, the domains S5 to S6 and the interconnecting loop complement into one central pore (Hoenderop et al. 2003; Gaudet 2008; Gees et al. 2012). In the last two decades, studies using a combination of site-directed mutagenesis, electrophysiology and structural modeling have clearly established that amino acids lining this central pore tune the Ca^{2+} selectivity of TRP channel pores, and that variability in this region can explain to a large extent the differences in Ca^{2+} permeability between TRP channels. For instance, mutation of a single aspartate in the pore loop of TRPV5 and TRPV6 to a non-charged residue changes the selectivity of these channels form Ca^{2+}-selective to non-selective (Nilius et al. 2001). Oppositely, mutation of a glutamine to a glutamate in the pore loop confers detectable Ca^{2+} permeability to TRPM4 (Nilius et al. 2005). Overall, the presence of negatively charged aspartate and glutamate residues in the pore loop was found to be a key determinant of Ca^{2+} permeability and

selectivity (Garcia-Martinez et al. 2000; Nilius et al. 2001; Hoenderop et al. 2003; Voets et al. 2003; Voets et al. 2004; Nilius et al. 2005; Owsianik et al. 2006).

To determine the contribution of a TRP channel to cellular Ca^{2+} signaling, not only the pore properties but also the gating mechanisms need to be taken into account. TRP channel gating can be induced by a wide variety of physical and chemical stimuli (Table 1), and the relative permeability to Ca^{2+} ions will crucially determine the cell physiological response to channel opening. Opening of Ca^{2+}-permeable non-selective TRP channels evokes a cytosolic Ca^{2+} rise as well as membrane depolarization, both of which can trigger cellular responses. For instance, several TRP channels are expressed in sensory endings of somatosensory neurons, where they respond to innocuous and noxious stimuli. There, opening of Ca^{2+}-permeable non-selective channels such as TRPA1, TRPV1 and TRPM3 not only causes depolarization that evokes action potential firing and propagation to the central nervous system to signal pain (Vandewauw et al. 2018), but also a local cytosolic Ca^{2+} rise that triggers neuropeptide release and neurogenic inflammation (Julius 2013). In the case of the Ca^{2+}-selective TRPV5 and TRPV6, the entry of Ca^{2+} ions lies at the basis of their role in the selective epithelial uptake, and transepithelial transport, of Ca^{2+} (Hoenderop et al. 2005). Depending on the cellular context, opening of the Ca^{2+}-impermeable TRPM4 and TRPM5 and the ensuing cell depolarization can either evoke, enhance or dampen cytosolic Ca^{2+} signals. On the one hand, depolarization promotes gating of voltage-gated Ca^{2+} channels present in most excitable cells. On the other hand, TRPM4- and TRPM5-mediated depolarization reduces the driving force for Ca^{2+} influx through both voltage-gated and voltage-independent (e.g. store-operated) Ca^{2+} channels, and can thus act as a break on Ca^{2+} entry (Liman 2007; Vennekens et al. 2007; Mathar et al. 2014).

To add to the complexity, a subset of TRP channels is functionally expressed at the membranes of intracellular organelles, including lysosomes and the endoplasmic reticulum (ER). Prominent example are the mucolipins (TRPML1, TRPML2 and TRPML3), which are predominantly found in organellar membranes. Mutations in TRPML1 cause the human lysosomal storage disease mucolipidosis type IV, and evidence is accumulating pointing at a crucial role for this channel in the transport of Ca^{2+} and other divalent cations across the lysosomal membrane as well as in lysosomal biogenesis and autophagy (Dong et al. 2008; Dong et al. 2010; Medina et al. 2015; Zhang et al. 2016). In addition, several TRP channels can be considered as non-committed TRP channels, as they can function in the plasma membrane as well as in intracellular membranes (Zhang et al. 2018a). A prominent example is TRPM2, which is best known as a plasma membrane channel activated by intracellular Ca^{2+} and intracellular ligands such ADP-ribose (ADPR), and by the recently discovered superagonist 2'-deoxy ADPR (Perraud et al. 2001; Sano et al. 2001; Fliegert et al. 2017), but can also

act as a lysosomal Ca^{2+}-release channel (Lange et al. 2009). A more elaborate review on intracellular TRP channels can be found elsewhere (Zhang et al. 2018a).

Cytosolic Ca^{2+} signals shaping TRP channel activity

Besides TRP channel gating shaping cellular Ca^{2+} signals, cytosolic Ca^{2+} itself also modulates the activity of several TRP channels. The action of Ca^{2+} on TRP channel gating can be both stimulatory and inhibitory, and can either be mediated via direct channel- Ca^{2+} interaction or alternatively involve cytosolic Ca^{2+}-binding proteins and/or Ca^{2+}-dependent signal transduction pathways (Fig. 2).

There are only a few examples in the literature of Ca^{2+}-binding sites in the cytosolic domains of TRP channels that have been proposed to contribute to direct effects of cytosolic Ca^{2+} on channel gating. These include an EF-hand structurein both the N-terminal domain of TRPA1 and in the cytosolic sside of the S1-S4 region in TRPM4 that have been implicated in Ca^{2+}-induced channel activation (Doerner et al. 2007; Zurborg et al. 2007; Autzen et al. 2018).

A more common means whereby Ca^{2+} can affect TRP channel activity involves cytosolic Ca^{2+}-binding proteins, with calmodulin (CaM) being the most prominent one. CaM-binding domains (CaMBDs) have been identified in the cytosolic regions of different TRP channels, including sites where CaM binds in the apo (Ca^{2+}-free) and Ca^{2+}-bound (Ca^{2+}-CaM) conformations. The effect of Ca^{2+}-CaM on TRP channel gating is channel dependent. For example, binding of Ca^{2+}-CaM to one of the CaMBDs located in the cytosolic N- or C-termini, underlies Ca^{2+}-dependent inactivation of TRP channels. This is exemplified by the highly Ca^{2+}-selective epithelial channels TRPV5 and TRPV6, where CaM-dependent inactivation functions as a fast feedback mechanism to maintain a tight Ca^{2+} homeostasis and prevent excessive Ca^{2+} influx (Kovalevskaya et al. 2012). In TRPV1, Ca^{2+}-CaM exerts a dual effect on channel desensitization, involving both a direct interaction with cytosolic CaMBDs as well as an indirect modulation via Ca^{2+}-CaM-dependent protein kinase II (CaMKII)-dependent channel phosphorylation (Bonnington and McNaughton 2003; Lau et al. 2012). In contrast, binding of Ca^{2+}-CaM to TRPV3 was proposed to sensitize the channel to repeated stimuli, although the underlying mechanism is unclear (Xiao et al. 2008). In addition to CaM, other Ca^{2+}-binding proteins have also been shown to interact with, and regulate, TRP channels. Examples include 80K-H and Calbindin-D28K interacting with TRPV5 (Lambers et al. 2006), and S100A1 interacting with TRPA1 and TRPM3 (Holakovska et al. 2012).

A third and frequently observed mechanism whereby Ca^{2+} affects TRP channel function is through activation of phospholipase C (PLC), which catalyzes the hydrolysis of phosphatidylinositol 4,5-bisphophate (PIP_2) in the plasma membrane into the second messengers inositol 1,4,5-trisphosphate (IP_3) and diacylglycerol (DAG) (Rohacs 2014). While some PLC isoforms are activated by G-protein

coupled receptors (GPCRs), others (PLCδ1, δ3 and δ4) can be activated by a rise in cytosolic Ca^{2+}, for instance upon TRP channel activation. For most TRP channels, PIP_2 acts as a positive regulator of channel activity, and consequently PIP_2 hydrolysis at the plasma membrane, whether through Ca^{2+}- or GPCR-dependent activation of PLC, causes channel desensitization; yet, there are also examples of inhibitory and bimodal effects of PIP_2 on TRP channel gating (Chuang et al. 2001; Lukacs et al. 2007; Zhang et al. 2012; Rohacs 2014).

A more elaborate review on the effect of Ca^{2+} on TRP channels can be found elsewhere (Hasan and Zhang 2018).

4. TRP channels entering the structural area

Given the varied and intricate interplay between TRP channels and cellular Ca^{2+} signaling, important questions have been raised regarding the interaction of TRP channels with Ca^{2+} and Ca^{2+}-regulated processes at the submolecular level. Such information is not only of fundamental interest, to elucidate the structural basis of the divergent permeability and gating properties of the different TRP channels, but also highly relevant to understand the pathophysiological consequences of disease-causing mutations in TRP channels and to develop specific pharmacological approaches for the treatment of TRP channel-related human diseases (Nilius et al. 2007; Nilius and Voets 2013).

- **The resolution revolution**

Although the first TRP gene was cloned in 1989 (Montell and Rubin 1989), it took almost 25 years until the first near-atomic-resolution TRP channel structure was resolved. Before that, high-resolution structural details were only available for a small number of specific intracellular domains of TRP channels (e.g. (Yamaguchi et al. 2001), and insights into the 3D-structure of entire TRP channels was limited to lower-resolution cryo-electron microscopy (cryo-EM) images, atomic force microscopy (e.g. (Barrera et al. 2007) (Gaudet 2008); (Moiseenkova-Bell and Wensel 2009)), and homology modelling using potassium channel structures as templates (e.g. (Kalia and Swartz 2013)). The lack of progress was partly due to difficulties in purifying membrane proteins into a stable, native protein conformation after removal from membrane detergents (Whited and Park 2014), as well as to the large cytoplasmic domains of TRP channels displaying significant flexibility and thereby hindering crystallization. Fortunately, recent advantages in cryo-EM, driven by developments in detectors and single particle analysis (Kuhlbrandt 2014), have led to a revolution in TRP channel structural biology (Madej and Ziegler 2018). In 2013, the side-chain resolution barrier was broken for the first time for membrane proteins without crystallization, when structures of TRPV1 were determined at a 3.4 Å resolution (Liao et al. 2013). This was achieved by combining a new, direct electron detector with novel image processing algorithms, thereby greatly improving the signal and correcting for motion-induced blurring. This accomplishment is regarded as a major breakthrough in the world of structural

biology and in the TRP channel field. These studies were the start of a resolution revolution, with an exponential increase in the number of structures of ion channels and other membrane proteins resolved at atomic detail (Kuhlbrandt 2014; Cheng 2015). As a result, detailed structures of at least one member of each TRP subfamily have been unraveled, providing insight into ion permeation and gating with resolution in the 3-4 Å-range (Table 2).

- **TRPV1 structures: a paradigm of TRP channel architecture and gating**

The cryo-EM structure of TRPV1 revealed an architecture characterized by a four-fold symmetry around a central ion permeation pore formed by transmembrane domains S5 to S6 and the intervening pore loop (S5-P-S6), surrounded by four independently folded modules composed of domains S1 to S4 (Liao et al. 2013). Overall, this architecture is very similar to that of voltage-gated K^+, Na^+ and Ca^{2+} channels (Kuang et al. 2015). The TRPV1 channel exhibits a wide extracellular mouth but a short selectivity filter, which sculpts the upper part of the gate (Liao et al. 2013). The conserved TRP domain that follows S6 interacts with the S4- S5 linker, which may facilitate coupling between different channel domains important for allosteric modulation. The assembly into tetramers is facilitated by interactions among cytoplasmic domains of the subunits. The ARD in the N-terminus is followed by a tightly packed linker that makes the connection with the pre-S1 helix.

These initial studies reported not only the structure of TRPV1 in its unliganded state (Liao et al. 2013), but also two structures obtained in the presence of ligand activators (Cao et al. 2013) allowing a first insight into possible structural rearrangements during channel gating. These ligand-bound TRPV1 structures included one obtained in the presence of the canonical vanilloid activator capsaicin, as well as one combining the ultrapotent vanilloid resiniferatoxin (RTX) with the double-knot toxin DkTx, which in functional assays traps the channel in a fully open state. In these structures, the vanilloid binding site was found buried in the channel complex in a binding pocket between the S4-S5 linker of one subunit and S6 of a neighboring subunit. In the RTX/DkTx-bound structure, four toxin moieties were observed atop each tetrameric channel complex. Each toxin binds at the extracellular loop of the outer pore region of one subunit and connects to the pore helix of a neighboring subunit (Cao et al. 2013).

By comparing the pore structures of TRPV1 in these three different conformational states, significant plasticity was noticed in the central pore, both at the level of the selectivity filter and at a lower region of the pore formed by S6. The funnel-like structure that comprises the pore starts with a rather wide outer pore, followed by a short selectivity filter. When the channel is in the unliganded state, the narrowest point of the filter, 4.6 Å, is created by two opposed carbonyl oxygens at position G643 (Liao et al. 2013). Further down the pore, the most constricted site is located at I679 (S6), where the distance between side chains measures 5.3 Å in the unliganded state (Liao et al. 2013). Upon vanilloid

binding, I679 rotates away from the central axis causing an expansion to 7.6 Å (Cao et al. 2013). In addition, in the RTX/DkTx structure, the pore helix tilts away from the central axis, thereby increasing the distance between the G643 carbonyls to 7.6 Å (Cao et al. 2013). Overall, these findings have led to the notion of a dual gating mechanism: in the unliganded conformation, both the upper and lower gate are constricted; the lower gate opens following vanilloid ligand binding; binding of DkTx, and possibly allosteric coupling with the lower gate, leads to additional opening of the upper gate.

- **A flurry of TRP channel structures**

Following the determination of TRPV1 structures using cryo-EM, similar approaches were successfully applied to many other members of the TRP channel superfamily. Moreover, by purifying TRP channels into lipid nanodiscs structural analysis of the channels in a more native, membrane-like environment has been achieved. Table 2 provides a summary of the published structures of TRP channels, with the cautionary note that this list is growing steadily.

At this point, structures of at least one member of every TRP channel subfamily are available, and representatives of each subfamily are represented in Figure 3. In general, these different TRP channels structures have a have several features, including a homotetrameric organization with fourfold symmetry, and a structurally conserved transmembrane organization that resembles that of other members of the superfamily of voltage-gated cation channels. One particular exception is the recent structure of a heterotetramer formed between the polycystic kidney disease-related PKD1 and TRPP1-PKD2 (Su et al. 2018a). Whereas TRPP1-PKD2 has all the features of a 6-TM TRP subunit and can form a homotetrameric channel, PKD1 is a much larger protein with an exoplasmic N-terminus and 11 transmembrane (TM)helices. Of these 11 TM domains, the last six show homology to the transmembrane segments of TRP channels, and one such subunit can apparently engage with three TRPP1-PKD2 subunits to form an asymmetric PKD1-PKD2 complex. However, the natural occurrence and functional properties of this complex remain to be established.

Despite common global architectures, there are several subfamily-specific features. In the exoplasmic region, TRPML and TRPP members exhibit a large structured domain formed by the S1-S2 linkers, known as the luminal domain (TRPML) and the polycystin domain (TRPP), which forms a fenestrated canopy-like structure atop the channel (Shen et al. 2016; Chen et al. 2017; Grieben et al. 2017; Hirschi et al. 2017; Schmiege et al. 2017). In contrast, members of the other subfamilies have only short and largely unstructured exoplasmic loops. In TRPA, TRPC and TRPV channels, the N-terminus contains multiple ankyrin repeats domains (ARD), which are implicated in protein-protein interaction, trafficking and gating. The number of ARDs ranges from three ARDs in TRPCs to 24 repeats in TRPA1. TRPM channels have relatively long N-termini but lack ARDs, as do the short N-

terminal tails of TRPP and TRPML channels. In their proximal C-terminus following the S6 helix, TRPC, TRPV and TRPM channels contain a highly conserved TRP domain, implicated in channel gating, which is not found in TRPA, TRPP and TRPML channels. At their distal C-terminal, three TRPM channels exhibit an integral enzyme domain: an atypical alpha-kinase in TRPM6 and TRPM7, and a NUDIX domain in TRPM2. Below, we highlight the structural features that specifically relate to Ca^{2+} permeation and TRP channel regulation by Ca^{2+}.

5. Structural insights into Ca^{2+} permeation

The central ion-conducting pore of TRP channels can be divided into an upper part, which forms the narrow selectivity filter lined by residues from the S5-S6 linker, and a lower part lined by residues from S6 that includes the lower gate. The lower gate is formed by hydrophobic residues that seal the lower part of the permeation pathway in the closed conformation, and rotate away to allow ion permeation upon channel activation. (Cao et al. 2013; Gao et al. 2016). This movement may be dependent on a short π-helical segment observed in the middle of S6, which has been suggested to facilitate helix bending during gating (Hughes et al. 2018b; Singh et al. 2018a). In addition to the lower gate, structural evidence has been provided for the existence of a second, upper gate at the level of the selectivity filter in some but not all TRP channels (Deng et al. 2018). However, the exact relevance of this upper gate to TRP channel gating and ion permeation is currently unclear.

A key question is whether the different TRP channel structures provide a framework to explain the large diversity in Ca^{2+} permeability properties of TRP channel pores. To address this, we here provide a comparison between the pores of TRP channels that reflect the entire range of Ca^{2+} permeability observed within the TRP superfamily (Fig. 1): the highly Ca^{2+}-selective TRPV6, the non-selective, Ca^{2+}-permeable TRPV1, and the Ca^{2+}-impermeable TRPM4 (Fig. 4).

The Ca^{2+}-selective pore of TRPV6

TRPV6 and its close homologue TRPV5 are the only two highly calcium-selective TRP channels, with estimated $P_{Ca^{2+}}/P_{Na^{+}}$ values >100 (Gunthorpe et al. 2002). Under normal ionic conditions, the inward current through TRPV6 is almost fully carried by Ca^{2+} ions (Nijenhuis et al. 2005). Earlier work combining structural modeling, the substituted cysteine accessibility method (SCAM) and patch-clamp recordings, had already established that a short stretch of amino acids in the S5-S6 linker, TIIDG, forms the selectivity filter (Nilius et al. 2001), with the aspartate residue (D541) forming the narrowest part of the open pore, with an estimated diameter of 5.4 Å. In addition, it was shown that substituting D541 (and the corresponding D542 in TRPV5) by a non-charged residue abolishes calcium-selectivity and block by other divalent cations (Voets et al. 2003). Many of these pre-structural findings were corroborated by recent structures obtained using both X-ray crystallography and cryo-EM. Indeed, crystal structures of TRPV6 obtained in the absence and presence of Ca^{2+}

confirm that the narrowest part of the pore is formed by the four side chains of D541, with a minimum interatomic distance of 4.6 Å, and that these aspartate side chains form a high-affinity site coordinating a single dehydrated Ca^{2+} ion (Saotome et al. 2016). Side-chain hydroxyls of T838 (also part of the TIIDG motif) participate in a second, lower affinity binding site for a dehydrated Ca^{2+} ion 6-8 Å below the ring of aspartates, whereas a third binding site in the vestibule below the selectivity filter may accommodate (partly) hydrated Ca^{2+}. Note that, similar to other highly Ca^{2+}-selective channels, TRPV6 permeates large currents carried by Na^+, K^+ and other monovalent cations in the absence of extracellular Ca^{2+} ions. In the wild type channel, these monovalent currents are blocked by low micromolar concentrations of Ca^{2+} or Cd^{2+}, and this inhibition is abolished when mutating D541 to a non-charged residue (Nilius et al. 2001).

Based on these results, a 'knock-off' mechanism of Ca^{2+} permeation was proposed (Saotome et al. 2016), where the binding of Ca^{2+} in electronegative ring formed by D541 side-chains is highly energetically favorable compared to the charge repulsion between the acidic side-chains in the unbound state. This implicates that removal of Ca^{2+} from this site leads to immediate replacement by another Ca^{2+} ion, a process that may be facilitated by recruitment of Ca^{2+} ions from the external solution by the highly electronegative extracellular vestibule of TRPV6. In the absence of extracellular Ca^{2+} ions, the ring of aspartates is no longer occupied by tightly bound Ca^{2+} ions, thus allowing large fluxes of monovalent cations.

Interestingly, comparison of the structures of the closed and open TRPV6 pore did not reveal any significant conformational changes at the level of the selectivity filter. In contrast, there was significant widening of the lower part of the pore lined by S6 residues, apparently induced by an α- to π- helical transition in the middle of S6 (McGoldrick et al. 2018). Therefore, in the case of TRPV6 the selectivity filter is static and solely involved in ion selectivity, whereas channel opening is controlled by a single (lower) gate.

The Ca^{2+}-permeable non-selective pore of TRPV1

TRPV1, like the related TRPV2-TRPV4 and the majority of other TRP channels (Owsianik et al. 2006), encompasses a pore that is non-selective for cations and shows significant Ca^{2+} permeability. Several studies report $P_{Ca^{2+}}/P_{Na^+}$ values for TRPV1 of approximately 10 (Caterina et al. 1997), and under physiological ionic conditions, approximately 10% of the inward current is carried by Ca^{2+} ions. Very similar permeability properties have been described for TRPV2-TRPV4.

The selectivity filter of these four Ca^{2+}-permeable non-selective TRPV channels contains the motif TIGMGD/E (Deng et al. 2018). Mutating the aspartate in TRPV1 to a non-charged residue significantly reduces $P_{Ca^{2+}}/P_{Na^+}$, indicative of the essential role of negative charges in the selectivity filter for Ca^{2+} permeation (Garcia-Martinez et al. 2000). However, in contrast to TRPV5 and TRPV6,

the negatively charged side chain is not located at the narrowest part of the pore, which instead is lined by neutral methionine side chains and backbone carbonyls (Liao et al. 2013). As a result, TRPV1 – TRPV4 lack a high-affinity Ca^{2+} binding site in the selectivity filter, thus explaining the poor discrimination between mono- and divalent cations. Note that in the unliganded state this narrowest constriction has a minimum diameter of 4.6 Å (Liao et al. 2013), which increases to 7.6 Å in the structure with RTX/DkTx (Cao et al. 2013). These dynamics at the level of the selectivity filter may contribute to the reported alterations in pore permeability properties upon strong stimulation of TRPV1, although further research is required to establish this.

The Ca^{2+}-impermeable pore of TRPM4

TRPM4 and the related TRPM5 are unique within the TRP superfamily in that they only conduct monovalent cations and are impermeable to Ca^{2+} (Liman 2007). Recent structures of TRPM4 reveal a normal ion-conducting pore with two constriction sites, similar to many other TRP channel structures. Although these structures do not clearly establish why TRPM4 fails to allow detectable permeation of Ca^{2+} ions, different mechanisms may contribute. First, the short but wide selectivity filter of TRPM4 consists of the motif FGQ, and thus does not contain any negatively charged amino acid, unlike other TRP channels (Winkler et al. 2017). Importantly, mutating the glutamine Q in the selectivity filter to a glutamate indeed resulted in detectable Ca^{2+} permeation through TRPM4 (Nilius et al. 2005), establishing the importance of negative charge. Nevertheless, TRPM2 and TRPM8 contain the same FGQ motif in their pore region, but are nonetheless able to permeate Ca^{2+}. A different selectivity filter configuration, as their pore loop is one amino acid shorter compared to TRPM4 and TRPM5, might explain this conundrum. Second, residues in the lower gate may also play a role in the monovalent ion selectivity. Interestingly, a serine that is shown to interact with permeating Na^{+} ions in the lower pore region is only conserved in TRPM4 and TRPM5, while other TRPM subfamily members contain an isoleucine at this position (Duan et al. 2018c). Note that TRPM4 contains negative charge at the top of the ion permeation pathway, just outside the selectivity filter. This electronegative mouth may serve to attract cations, but the local negative charge is likely not strong enough to promote dehydration of divalent cations, which is necessary to permeate the pore (Duan et al. 2018c).

6. Structural insights into Ca^{2+} regulation

In addition to these insights into the ion permeation pathway, recent TRP channel structures also provide interesting novel structural clues towards understanding Ca^{2+}-dependent processes that regulate channel gating (Figs. 2, 5).

Intracellular Ca^{2+} binding site in TRP channels

The activity of several members of the TRPM subfamily is enhanced by a direct binding of Ca^{2+} ions to the channel protein. In particular, the Ca^{2+}-impermeable TRPM4 and TRPM5 are activated by a cytosolic Ca^{2+} rise in a voltage-dependent manner. Cryo-EM structures of TRPM4 were obtained in both Ca^{2+}-bound and unbound conformations, revealing a Ca^{2+}-binding site located at, and coordinated by, side chains of transmembrane domains S2 and S3 (Autzen et al. 2018) (Fig. 5). Based on these structures, Ca^{2+} binding to TRPM4 triggers a cascade of small conformational effects throughout the whole channel, in order to prime the channel for voltage-dependent opening.

Interestingly, several of the residues implicated in Ca^{2+} binding in TRPM4 are conserved only in other members of the TRPM family that show Ca^{2+}-dependent gating, namely TRPM2, TRPM5 and TRPM8. Moreover a high-resolution structure of the ADPR-activated TRPM2 channel in the presence of Ca^{2+} (Huang et al. 2018; Wang et al. 2018) revealed, similar to TRPM4, a Ca^{2+}-binding site at the cytosolic side of S2 and S3 of both the human and the zebrafish TRPM2 orthologs (Fliegert et al. 2018). Structural comparison with the apo structure indicates a repositioning of S3 upon Ca^{2+} binding, enabling movement of the S4-S5 linker to facilitate activation. At the functional level, earlier studies showed that mutation of residues in this region indeed impairs activation of TRPM2 in the presence of Ca^{2+} (Winking et al. 2012). Although structural data to confirm this are not yet available, is likely that this cytosolic Ca^{2+}-binding site is also present in TRPM5 and TRPM8. In support of this notion, mutations of the corresponding amino acids in TRPM8 abolish the Ca^{2+}-dependent activation by icilin, while leaving responses to cold and menthol intact (Chuang et al. 2004).

In addition to these TRPM channels, structural evidence has also been provided for intracellular Ca^{2+}-binding sites in other TRP channels, including a well-defined EF-hand in the proximal C-terminus of TRPP1-PKD2, implicated in Ca^{2+}-dependent activation of the channel (Yang et al. 2016; Grieben et al. 2017; Wilkes et al. 2017).

Cytosolic interactions between TRPV channels and Ca^{2+}-CaM

CaM consists of two globular domains, connected by a flexible linker. Two Ca^{2+} ions can bind to the EF-hand motifs of every domain, resulting in a maximum of four Ca^{2+} ions bound to a single CaM. Ca^{2+} binding induces a conformational change in the backbone of CaM, allowing interaction with a wide range of target proteins, including TRP channels. The number of TRP channels interacting with CaM is large (see http://trpchannel.org/proteins/show?id=Calmodulin), and the effects it can trigger are equally diverse. Furthermore, there can be multiple CaM interaction sites within one TRP channel, where binding can mediate divergent effects on channel function (Zhu 2005).

The first high-resolution insights into CaM-TRP channel interactions were provided by a crystal structure of Ca^{2+}-bound CaM in complex with a 35-residue C-terminal segment of TRPV1 (Lau et al. 2012). This study revealed that CaM clasps around the helical C-terminus of TRPV1 in a Ca^{2+}-

dependent manner, and that disruption of the interaction slows Ca^{2+}-dependent channel desensitization, although a second CaM-interaction site in the N-terminus was found that plays a more prominent role in this process.

Recently, structures were determined for the full-length TRPV5 and TRPV6 in a complex with Ca^{2+}-bound CaM (Hughes et al. 2018b; Singh et al. 2018b). In the structure of TRPV5 saturated with Ca^{2+}-CaM, both lobes of CaM interact with different sections of the C-terminus via numerous hydrophobic contacts (Hughes et al. 2018b). This results in an occupation of the tryptophan amino acids in the lower gate of TRPV5, directly obstructing ion permeation (Figure 5). The critical role of this interaction in Ca^{2+}-CaM-mediated effects was established in functional studies showing that mutating the critical tryptophan residues abolishes Ca^{2+}-CaM-dependent channel inhibition. This mechanism represents an important negative feedback loop that regulates calcium influx in Ca^{2+}-reabsorbing epithelia. A very similar structural mechanism has been put forward for the close homologue TRPV6, as structures showed a comparable binding of CaM to the C terminus of TRPV6, with the C-lobe of CaM inserted into the pore's intracellular entrance (Singh et al. 2018b). There is currently insufficient structural information to establish whether this mechanism is conserved in other TRP channels.

TRP channel interactions with PIP_2

The level of PIP_2, the most abundant phosphoinositide in the inner leaflet of the plasma membrane of mammalian cells, is typically around 1% of total plasma membrane anionic phospholipids (Czech 2000). Despite being a minor constituent of the plasma membrane, PIP_2 has a major impact on the functioning of many, if not all TRP channels (Voets and Nilius 2007). Both a rise in intracellular Ca^{2+} levels, acting via Ca^{2+}-dependent PLC (see above), as well as activation of PLC downstream of GPCRs and receptor tyrosine kinases, can result in a rapid decrease in PIP_2 levels, constituting a common and powerful mechanism of TRP channel regulation (Rohacs 2014). Most TRP channels are inhibited when PIP_2 levels decrease, although inhibitory effects of PIP_2 have also been observed in some TRP channels (Qin 2007; Rohacs 2014). Recently, by combining cryo-EM with nanodisc technology, several structures have been obtained of TRP channels in a biological membrane-like environment, allowing structural characterisation of PIP_2 interaction sites.

In the case of TRPV1, a PIP_2 molecule was identified in the binding pocket for vanilloids such as capsaicin and RTX, suggesting that these activating ligands must displace PIP_2 to bind and activate the channel. A cryo-EM structure of TRPV5 in the presence of PIP_2 revealed a single PIP_2 molecule interacting with the N-linker, the S4-S5 linker and the S6 helix of the channel (Hughes et al. 2018b), a finding that correlated with molecular dynamics (MD) predictions of a PIP_2 binding site in the close homologue TRPV6 (Fig. 5). Comparing structures of TRPV5 with and without bound PIP_2 revealed

important conformational rearrangements in the channel (Hughes et al. 2018b). Upon binding of PIP_2 the aspartate residues in the selectivity filter change orientation, clearing the initial road of the ion-conducting pathway. In addition, the lower gate of the pore extends wide enough to allow the flow of hydrated Ca^{2+} ions. These results form a beautiful example of how high-resolution structures can elucidate previously mysterious mechanisms of TRP channel regulation.

7. Conclusion and outlook

TRP channel research benefited greatly from the recent resolution revolution. TRPV1 was the first full-length high-resolution membrane protein structure that was unraveled without the need for crystallizing the protein, representing a milestone for the fields of structural biology and TRP channel biology alike.

Thanks to the growing number of channel structures, including members of every TRP subfamily, subgroup, we are now able to visualize different conformational states leading to channel gating, rationalize ion permeation and define the details of TRP channel interactions with regulatory proteins, lipids and ions. In this review, we have selectively highlighted novel insights related to Ca^{2+} permeation and Ca^{2+}-dependent regulation of these channels. Undoubtedly, these novel insights and further structural work will not only fuel fundamental research into TRP channel function and regulation, but also increase our understanding of the etiology of TRP channel-related human diseases and assist in the rational design of pharmacological therapies for such diseases.

References

Arias-Darraz L, Cabezas D, Colenso CK, Alegria-Arcos M, Bravo-Moraga F, Varas-Concha I, Almonacid DE, Madrid R, Brauchi S. 2015. A transient receptor potential ion channel in Chlamydomonas shares key features with sensory transduction-associated TRP channels in mammals. *Plant Cell* **27**: 177-188.

Autzen HE, Myasnikov AG, Campbell MG, Asarnow D, Julius D, Cheng Y. 2018. Structure of the human TRPM4 ion channel in a lipid nanodisc. *Science* **359**: 228-232.

Barrera NP, Shaifta Y, McFadzean I, Ward JP, Henderson RM, Edwardson JM. 2007. AFM imaging reveals the tetrameric structure of the TRPC1 channel. *Biochem Biophys Res Commun* **358**: 1086-1090.

Berridge MJ. 2017. Calcium signalling in health and disease. *Biochem Biophys Res Commun* **485**: 5.

Bonnington JK, McNaughton PA. 2003. Signalling pathways involved in the sensitisation of mouse nociceptive neurones by nerve growth factor. *J Physiol* **551**: 433-446.

Cao E, Liao M, Cheng Y, Julius D. 2013. TRPV1 structures in distinct conformations reveal activation mechanisms. *Nature* **504**: 113-118.

Caterina MJ, Schumacher MA, Tominaga M, Rosen TA, Levine JD, Julius D. 1997. The capsaicin receptor: a heat-activated ion channel in the pain pathway. *Nature* **389**: 816-824.

Chen Q, She J, Zeng W, Guo J, Xu H, Bai XC, Jiang Y. 2017. Structure of mammalian endolysosomal TRPML1 channel in nanodiscs. *Nature* **550**: 415-418.

Cheng Y. 2015. Single-Particle Cryo-EM at Crystallographic Resolution. *Cell* **161**: 450-457.

Chuang HH, Neuhausser WM, Julius D. 2004. The super-cooling agent icilin reveals a mechanism of coincidence detection by a temperature-sensitive TRP channel. *Neuron* **43**: 859-869.

Chuang HH, Prescott ED, Kong H, Shields S, Jordt SE, Basbaum AI, Chao MV, Julius D. 2001. Bradykinin and nerve growth factor release the capsaicin receptor from PtdIns(4,5)P2-mediated inhibition. *Nature* **411**: 957-962.

Clapham DE. 2003. TRP channels as cellular sensors. *Nature* **426**: 517-524.

Czech MP. 2000. PIP2 and PIP3: complex roles at the cell surface. *Cell* **100**: 603-606.

Deng Z, Paknejad N, Maksaev G, Sala-Rabanal M, Nichols CG, Hite RK, Yuan P. 2018. Cryo-EM and X-ray structures of TRPV4 reveal insight into ion permeation and gating mechanisms. *Nat Struct Mol Biol* **25**: 252-260.

Doerner JF, Gisselmann G, Hatt H, Wetzel CH. 2007. Transient receptor potential channel A1 is directly gated by calcium ions. *J Biol Chem* **282**: 13180-13189.

Dong XP, Cheng X, Mills E, Delling M, Wang F, Kurz T, Xu H. 2008. The type IV mucolipidosis-associated protein TRPML1 is an endolysosomal iron release channel. *Nature* **455**: 992-996.

Dong XP, Shen D, Wang X, Dawson T, Li X, Zhang Q, Cheng X, Zhang Y, Weisman LS, Delling M et al. 2010. PI(3,5)P(2) controls membrane trafficking by direct activation of mucolipin Ca(2+) release channels in the endolysosome. *Nat Commun* **1**: 38.

Dosey TL, Wang Z, Fan G, Zhang Z, Serysheva II, Chiu W, Wensel TG. 2018. TRPV2 Ion Channel Gating Through Allosteric Domain Coupling Revealed by Cryo-EM . . *Available at SSRN* **http://dx.doi.org/10.2139/ssrn.3155836**.

Duan J, Li J, Zeng B, Chen GL, Peng X, Zhang Y, Wang J, Clapham DE, Li Z, Zhang J. 2018a. Structure of the mouse TRPC4 ion channel. *Nat Commun* **9**: 3102.

Duan J, Li Z, Li J, Hulse RE, Santa-Cruz A, Valinsky WC, Abiria SA, Krapivinsky G, Zhang J, Clapham DE. 2018b. Structure of the mammalian TRPM7, a magnesium channel required during embryonic development. *Proc Natl Acad Sci U S A* **115**: E8201-E8210.

Duan J, Li Z, Li J, Santa-Cruz A, Sanchez-Martinez S, Zhang J, Clapham DE. 2018c. Structure of full-length human TRPM4. *Proc Natl Acad Sci U S A* **115**: 2377-2382.

Fan C, Choi W, Sun W, Du J, Lu W. 2018. Structure of the human lipid-gated cation channel TRPC3. *Elife* **7**.

Fine M, Schmiege P, Li X. 2018. Structural basis for PtdInsP2-mediated human TRPML1 regulation. *Nat Commun* **9**: 4192.

Fliegert R, Bauche A, Wolf Perez AM, Watt JM, Rozewitz MD, Winzer R, Janus M, Gu F, Rosche A, Harneit A et al. 2017. 2'-Deoxyadenosine 5'-diphosphoribose is an endogenous TRPM2 superagonist. *Nat Chem Biol* **13**: 1036-1044.
Fliegert R, Holzer HT, Guse AH. 2018. TRPM2 activation: Paradigm shifted? *Cell Calcium*.
Gao Y, Cao E, Julius D, Cheng Y. 2016. TRPV1 structures in nanodiscs reveal mechanisms of ligand and lipid action. *Nature* **534**: 347-351.
Garcia-Martinez C, Morenilla-Palao C, Planells-Cases R, Merino JM, Ferrer-Montiel A. 2000. Identification of an aspartic residue in the P-loop of the vanilloid receptor that modulates pore properties. *J Biol Chem* **275**: 32552-32558.
Gaudet R. 2008. TRP channels entering the structural era. *J Physiol* **586**: 3565-3575.
Gees M, Owsianik G, Nilius B, Voets T. 2012. TRP channels. *Compr Physiol* **2**: 563-608.
Grieben M, Pike AC, Shintre CA, Venturi E, El-Ajouz S, Tessitore A, Shrestha L, Mukhopadhyay S, Mahajan P, Chalk R et al. 2017. Structure of the polycystic kidney disease TRP channel Polycystin-2 (PC2). *Nat Struct Mol Biol* **24**: 114-122.
Gunthorpe MJ, Benham CD, Randall A, Davis JB. 2002. The diversity in the vanilloid (TRPV) receptor family of ion channels. *Trends Pharmacol Sci* **23**: 183-191.
Guo J, She J, Zeng W, Chen Q, Bai XC, Jiang Y. 2017. Structures of the calcium-activated, non-selective cation channel TRPM4. *Nature* **552**: 205-209.
Harteneck C, Plant TD, Schultz G. 2000. From worm to man: three subfamilies of TRP channels. *Trends Neurosci* **23**: 159-166.
Hasan R, Zhang X. 2018. Ca(2+) Regulation of TRP Ion Channels. *Int J Mol Sci* **19**.
Hirschi M, Herzik MA, Jr., Wie J, Suo Y, Borschel WF, Ren D, Lander GC, Lee SY. 2017. Cryo-electron microscopy structure of the lysosomal calcium-permeable channel TRPML3. *Nature* **550**: 411-414.
Hoenderop JG, Nilius B, Bindels RJ. 2005. Calcium absorption across epithelia. *Physiol Rev* **85**: 373-422.
Hoenderop JG, Voets T, Hoefs S, Weidema F, Prenen J, Nilius B, Bindels RJ. 2003. Homo- and heterotetrameric architecture of the epithelial Ca2+ channels TRPV5 and TRPV6. *EMBO J* **22**: 776-785.
Holakovska B, Grycova L, Jirku M, Sulc M, Bumba L, Teisinger J. 2012. Calmodulin and S100A1 protein interact with N terminus of TRPM3 channel. *J Biol Chem* **287**: 16645-16655.
Huang Y, Winkler PA, Sun W, Lu W, Du J. 2018. Architecture of the TRPM2 channel and its activation mechanism by ADP-ribose and calcium. *Nature*.
Hughes TET, Lodowski DT, Huynh KW, Yazici A, Del Rosario J, Kapoor A, Basak S, Samanta A, Han X, Chakrapani S et al. 2018a. Structural basis of TRPV5 channel inhibition by econazole revealed by cryo-EM. *Nat Struct Mol Biol* **25**: 53-60.
Hughes TET, Pumroy RA, Yazici AT, Kasimova MA, Fluck EC, Huynh KW, Samanta A, Molugu SK, Zhou ZH, Carnevale V et al. 2018b. Structural insights on TRPV5 gating by endogenous modulators. *Nat Commun* **9**: 4198.
Hulse RE, Li Z, Huang RK, Zhang J, Clapham DE. 2018. Cryo-EM structure of the polycystin 2-l1 ion channel. *Elife* **7**.
Huynh KW, Cohen MR, Jiang J, Samanta A, Lodowski DT, Zhou ZH, Moiseenkova-Bell VY. 2016. Structure of the full-length TRPV2 channel by cryo-EM. *Nat Commun* **7**: 11130.
Julius D. 2013. TRP channels and pain. *Annu Rev Cell Dev Biol* **29**: 355-384.
Kalia J, Swartz KJ. 2013. Exploring structure-function relationships between TRP and Kv channels. *Sci Rep* **3**: 1523.
Kovalevskaya NV, Bokhovchuk FM, Vuister GW. 2012. The TRPV5/6 calcium channels contain multiple calmodulin binding sites with differential binding properties. *J Struct Funct Genomics* **13**: 91-100.
Kuang Q, Purhonen P, Hebert H. 2015. Structure of potassium channels. *Cell Mol Life Sci* **72**: 3677-3693.
Kuhlbrandt W. 2014. Biochemistry. The resolution revolution. *Science* **343**: 1443-1444.
Lambers TT, Mahieu F, Oancea E, Hoofd L, de Lange F, Mensenkamp AR, Voets T, Nilius B, Clapham DE, Hoenderop JG et al. 2006. Calbindin-D28K dynamically controls TRPV5-mediated Ca2+ transport. *EMBO J* **25**: 2978-2988.
Lange I, Yamamoto S, Partida-Sanchez S, Mori Y, Fleig A, Penner R. 2009. TRPM2 functions as a lysosomal Ca2+-release channel in beta cells. *Sci Signal* **2**: ra23.

Lau SY, Procko E, Gaudet R. 2012. Distinct properties of Ca2+-calmodulin binding to N- and C-terminal regulatory regions of the TRPV1 channel. *J Gen Physiol* **140**: 541-555.
Launay P, Fleig A, Perraud AL, Scharenberg AM, Penner R, Kinet JP. 2002. TRPM4 is a Ca2+-activated nonselective cation channel mediating cell membrane depolarization. *Cell* **109**: 397-407.
Liao M, Cao E, Julius D, Cheng Y. 2013. Structure of the TRPV1 ion channel determined by electron cryo-microscopy. *Nature* **504**: 107-112.
Liman ER. 2007. The Ca(2+)-Activated TRP Channels: TRPM4 and TRPM5. in *TRP Ion Channel Function in Sensory Transduction and Cellular Signaling Cascades* (eds. WB Liedtke, S Heller), Boca Raton (FL).
Lukacs V, Thyagarajan B, Varnai P, Balla A, Balla T, Rohacs T. 2007. Dual regulation of TRPV1 by phosphoinositides. *J Neurosci* **27**: 7070-7080.
Madej MG, Ziegler CM. 2018. Dawning of a new era in TRP channel structural biology by cryo-electron microscopy. *Pflugers Arch* **470**: 213-225.
Mathar I, Jacobs G, Kecskes M, Menigoz A, Philippaert K, Vennekens R. 2014. Trpm4. *Handb Exp Pharmacol* **222**: 461-487.
McGoldrick LL, Singh AK, Saotome K, Yelshanskaya MV, Twomey EC, Grassucci RA, Sobolevsky AI. 2018. Opening of the human epithelial calcium channel TRPV6. *Nature* **553**: 233-237.
Medina DL, Di Paola S, Peluso I, Armani A, De Stefani D, Venditti R, Montefusco S, Scotto-Rosato A, Prezioso C, Forrester A et al. 2015. Lysosomal calcium signalling regulates autophagy through calcineurin and TFEB. *Nat Cell Biol* **17**: 288-299.
Minke B, Wu C, Pak WL. 1975. Induction of photoreceptor voltage noise in the dark in Drosophila mutant. *Nature* **258**: 84-87.
Moiseenkova-Bell VY, Wensel TG. 2009. Hot on the trail of TRP channel structure. *J Gen Physiol* **133**: 239-244.
Montell C, Rubin GM. 1989. Molecular characterization of the Drosophila trp locus: a putative integral membrane protein required for phototransduction. *Neuron* **2**: 1313-1323.
Mulier M, Vriens J, Voets T. 2017. TRP channel pores and local calcium signals. *Cell Calcium* **66**: 19-24.
Nijenhuis T, Hoenderop JG, Bindels RJ. 2005. TRPV5 and TRPV6 in Ca(2+) (re)absorption: regulating Ca(2+) entry at the gate. *Pflugers Arch* **451**: 181-192.
Nilius B, Owsianik G, Voets T, Peters JA. 2007. Transient receptor potential cation channels in disease. *Physiol Rev* **87**: 165-217.
Nilius B, Prenen J, Janssens A, Owsianik G, Wang C, Zhu MX, Voets T. 2005. The selectivity filter of the cation channel TRPM4. *J Biol Chem* **280**: 22899-22906.
Nilius B, Vennekens R, Prenen J, Hoenderop JG, Droogmans G, Bindels RJ. 2001. The single pore residue Asp542 determines Ca2+ permeation and Mg2+ block of the epithelial Ca2+ channel. *J Biol Chem* **276**: 1020-1025.
Nilius B, Voets T. 2013. The puzzle of TRPV4 channelopathies. *EMBO Rep* **14**: 152-163.
Owsianik G, Talavera K, Voets T, Nilius B. 2006. Permeation and selectivity of TRP channels. *Annu Rev Physiol* **68**: 685-717.
Paulsen CE, Armache JP, Gao Y, Cheng Y, Julius D. 2015. Structure of the TRPA1 ion channel suggests regulatory mechanisms. *Nature* **525**: 552.
Perraud AL, Fleig A, Dunn CA, Bagley LA, Launay P, Schmitz C, Stokes AJ, Zhu Q, Bessman MJ, Penner R et al. 2001. ADP-ribose gating of the calcium-permeable LTRPC2 channel revealed by Nudix motif homology. *Nature* **411**: 595-599.
Prawitt D, Monteilh-Zoller MK, Brixel L, Spangenberg C, Zabel B, Fleig A, Penner R. 2003. TRPM5 is a transient Ca2+-activated cation channel responding to rapid changes in [Ca2+]i. *Proc Natl Acad Sci U S A* **100**: 15166-15171.
Qin F. 2007. Regulation of TRP ion channels by phosphatidylinositol-4,5-bisphosphate. *Handb Exp Pharmacol*: 509-525.
Rohacs T. 2014. Phosphoinositide regulation of TRP channels. *Handb Exp Pharmacol* **223**: 1143-1176.
Sano Y, Inamura K, Miyake A, Mochizuki S, Yokoi H, Matsushime H, Furuichi K. 2001. Immunocyte Ca2+ influx system mediated by LTRPC2. *Science* **293**: 1327-1330.
Saotome K, Singh AK, Yelshanskaya MV, Sobolevsky AI. 2016. Crystal structure of the epithelial calcium channel TRPV6. *Nature* **534**: 506-511.

Schmiege P, Fine M, Blobel G, Li X. 2017. Human TRPML1 channel structures in open and closed conformations. *Nature* **550**: 366-370.
Shen PS, Yang X, DeCaen PG, Liu X, Bulkley D, Clapham DE, Cao E. 2016. The Structure of the Polycystic Kidney Disease Channel PKD2 in Lipid Nanodiscs. *Cell* **167**: 763-773 e711.
Sierra-Valdez F, Azumaya CM, Romero LO, Nakagawa T, Cordero-Morales JF. 2018. Structure-function analyses of the ion channel TRPC3 reveal that its cytoplasmic domain allosterically modulates channel gating. *J Biol Chem* **293**: 16102-16114.
Singh AK, McGoldrick LL, Sobolevsky AI. 2018a. Structure and gating mechanism of the transient receptor potential channel TRPV3. *Nat Struct Mol Biol*.
Singh AK, McGoldrick LL, Twomey EC, Sobolevsky AI. 2018b. Mechanism of calmodulin inactivation of the calcium-selective TRP channel TRPV6. *Sci Adv* **4**: eaau6088.
Singh AK, Saotome K, McGoldrick LL, Sobolevsky AI. 2018c. Structural bases of TRP channel TRPV6 allosteric modulation by 2-APB. *Nat Commun* **9**: 2465.
Su Q, Hu F, Ge X, Lei J, Yu S, Wang T, Zhou Q, Mei C, Shi Y. 2018a. Structure of the human PKD1/PKD2 complex. *Science*.
Su Q, Hu F, Liu Y, Ge X, Mei C, Yu S, Shen A, Zhou Q, Yan C, Lei J et al. 2018b. Cryo-EM structure of the polycystic kidney disease-like channel PKD2L1. *Nat Commun* **9**: 1192.
Tang Q, Guo W, Zheng L, Wu JX, Liu M, Zhou X, Zhang X, Chen L. 2018. Structure of the receptor-activated human TRPC6 and TRPC3 ion channels. *Cell Res* **28**: 746-755.
Vandewauw I, De Clercq K, Mulier M, Held K, Pinto S, Van Ranst N, Segal A, Voet T, Vennekens R, Zimmermann K et al. 2018. A TRP channel trio mediates acute noxious heat sensing. *Nature* **555**: 662-666.
Venkatachalam K, Montell C. 2007. TRP channels. *Annu Rev Biochem* **76**: 387-417.
Vennekens R, Hoenderop JG, Prenen J, Stuiver M, Willems PH, Droogmans G, Nilius B, Bindels RJ. 2000. Permeation and gating properties of the novel epithelial Ca(2+) channel. *J Biol Chem* **275**: 3963-3969.
Vennekens R, Olausson J, Meissner M, Bloch W, Mathar I, Philipp SE, Schmitz F, Weissgerber P, Nilius B, Flockerzi V et al. 2007. Increased IgE-dependent mast cell activation and anaphylactic responses in mice lacking the calcium-activated nonselective cation channel TRPM4. *Nat Immunol* **8**: 312-320.
Vinayagam D, Mager T, Apelbaum A, Bothe A, Merino F, Hofnagel O, Gatsogiannis C, Raunser S. 2018. Electron cryo-microscopy structure of the canonical TRPC4 ion channel. *Elife* **7**.
Voets T, Janssens A, Droogmans G, Nilius B. 2004. Outer pore architecture of a Ca2+-selective TRP channel. *J Biol Chem* **279**: 15223-15230.
Voets T, Janssens A, Prenen J, Droogmans G, Nilius B. 2003. Mg2+-dependent gating and strong inward rectification of the cation channel TRPV6. *J Gen Physiol* **121**: 245-260.
Voets T, Nilius B. 2007. Modulation of TRPs by PIPs. *J Physiol* **582**: 939-944.
Wang L, Fu TM, Zhou Y, Xia S, Greka A, Wu H. 2018. Structures and gating mechanism of human TRPM2. *Science*.
Whited AM, Park PS. 2014. Atomic force microscopy: a multifaceted tool to study membrane proteins and their interactions with ligands. *Biochim Biophys Acta* **1838**: 56-68.
Wilkes M, Madej MG, Kreuter L, Rhinow D, Heinz V, De Sanctis S, Ruppel S, Richter RM, Joos F, Grieben M et al. 2017. Molecular insights into lipid-assisted Ca(2+) regulation of the TRP channel Polycystin-2. *Nat Struct Mol Biol* **24**: 123-130.
Winking M, Hoffmann DC, Kuhn C, Hilgers RD, Luckhoff A, Kuhn FJ. 2012. Importance of a conserved sequence motif in transmembrane segment S3 for the gating of human TRPM8 and TRPM2. *PLoS One* **7**: e49877.
Winkler PA, Huang Y, Sun W, Du J, Lu W. 2017. Electron cryo-microscopy structure of a human TRPM4 channel. *Nature* **552**: 200-204.
Xiao R, Tang J, Wang C, Colton CK, Tian J, Zhu MX. 2008. Calcium plays a central role in the sensitization of TRPV3 channel to repetitive stimulations. *J Biol Chem* **283**: 6162-6174.
Yamaguchi H, Matsushita M, Nairn AC, Kuriyan J. 2001. Crystal structure of the atypical protein kinase domain of a TRP channel with phosphotransferase activity. *Mol Cell* **7**: 1047-1057.
Yang Y, Hodsdon ME, Lolis EJ, Ehrlich BE. 2016. Conformational dynamics of Ca2+-dependent responses in the polycystin-2 C-terminal tail. *Biochem J* **473**: 285-296.
Yin Y, Wu M, Zubcevic L, Borschel WF, Lander GC, Lee SY. 2018. Structure of the cold- and menthol-sensing ion channel TRPM8. *Science* **359**: 237-241.

Yu FH, Catterall WA. 2004. The VGL-chanome: a protein superfamily specialized for electrical signaling and ionic homeostasis. *Sci STKE* **2004**: re15.
Yue L, Peng JB, Hediger MA, Clapham DE. 2001. CaT1 manifests the pore properties of the calcium-release-activated calcium channel. *Nature* **410**: 705-709.
Zhang S, Li N, Zeng W, Gao N, Yang M. 2017. Cryo-EM structures of the mammalian endo-lysosomal TRPML1 channel elucidate the combined regulation mechanism. *Protein Cell* **8**: 834-847.
Zhang X, Cheng X, Yu L, Yang J, Calvo R, Patnaik S, Hu X, Gao Q, Yang M, Lawas M et al. 2016. MCOLN1 is a ROS sensor in lysosomes that regulates autophagy. *Nat Commun* **7**: 12109.
Zhang X, Hu M, Yang Y, Xu H. 2018a. Organellar TRP channels. *Nat Struct Mol Biol* **25**: 1009-1018.
Zhang X, Li X, Xu H. 2012. Phosphoinositide isoforms determine compartment-specific ion channel activity. *Proc Natl Acad Sci U S A* **109**: 11384-11389.
Zhang Z, Toth B, Szollosi A, Chen J, Csanady L. 2018b. Structure of a TRPM2 channel in complex with Ca(2+) explains unique gating regulation. *Elife* **7**.
Zheng W, Yang X, Hu R, Cai R, Hofmann L, Wang Z, Hu Q, Liu X, Bulkey D, Yu Y et al. 2018. Hydrophobic pore gates regulate ion permeation in polycystic kidney disease 2 and 2L1 channels. *Nat Commun* **9**: 2302.
Zhou X, Li M, Su D, Jia Q, Li H, Li X, Yang J. 2017. Cryo-EM structures of the human endolysosomal TRPML3 channel in three distinct states. *Nat Struct Mol Biol* **24**: 1146-1154.
Zhu MX. 2005. Multiple roles of calmodulin and other Ca(2+)-binding proteins in the functional regulation of TRP channels. *Pflugers Arch* **451**: 105-115.
Zubcevic L, Herzik MA, Jr., Chung BC, Liu Z, Lander GC, Lee SY. 2016. Cryo-electron microscopy structure of the TRPV2 ion channel. *Nat Struct Mol Biol* **23**: 180-186.
Zubcevic L, Herzik MA, Jr., Wu M, Borschel WF, Hirschi M, Song AS, Lander GC, Lee SY. 2018a. Conformational ensemble of the human TRPV3 ion channel. *Nat Commun* **9**: 4773.
Zubcevic L, Le S, Yang H, Lee SY. 2018b. Conformational plasticity in the selectivity filter of the TRPV2 ion channel. *Nat Struct Mol Biol* **25**: 405-415.
Zurborg S, Yurgionas B, Jira JA, Caspani O, Heppenstall PA. 2007. Direct activation of the ion channel TRPA1 by Ca2+. *Nat Neurosci* **10**: 277-279.

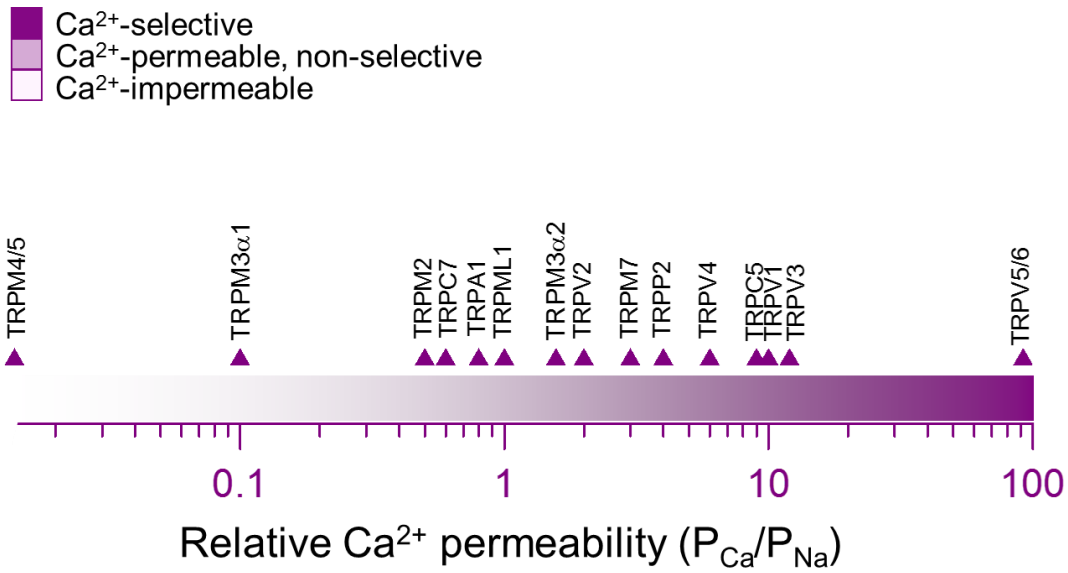

Figure 1: Ca^{2+} permeability of TRP channels. On a logarithmic scale, examples of the indicated mammalian TRP channels illustrating the range of relative Ca^{2+} permeabilities (based on reversal potential measurements).

Note that values are indicative, as the obtained values can vary significantly depending on cellular environment and experimental conditions.

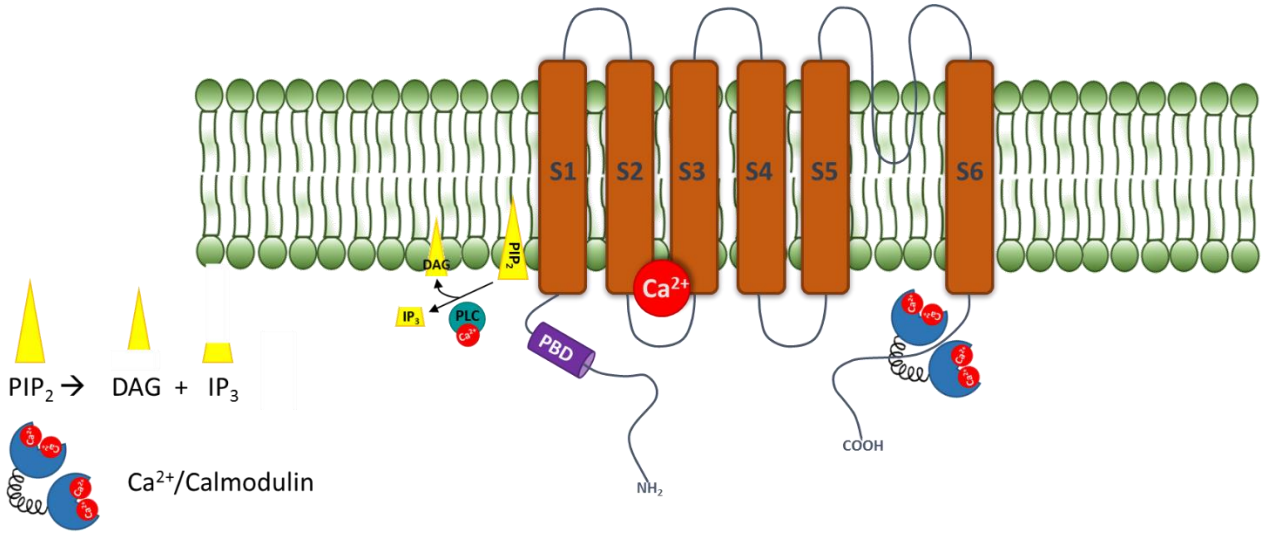

Figure 2: Cartoon illustrating three general mechanisms of Ca^{2+}-dependent regulation of TRP channel activity. Left: Ca^{2+} (red spheres) can cause a decrease in the plasma membrane PIP_2 levels via Ca^{2+}-activated phospholipase C. This decrease is sensed by PIP_2-binding domains (PBD, purple), which are found at various locations in the cytosolic part of TRP channels. Center: Ca^{2+} can bind directly to activate TRP channels, for instance via residues in the S2-S3 region of TRPM channels. Right: Ca^{2+} can influence TRP channel activity via Calmodulin (CaM, blue), for example via Ca^{2+}-CaM-binding in the C terminus of TRPV channels.

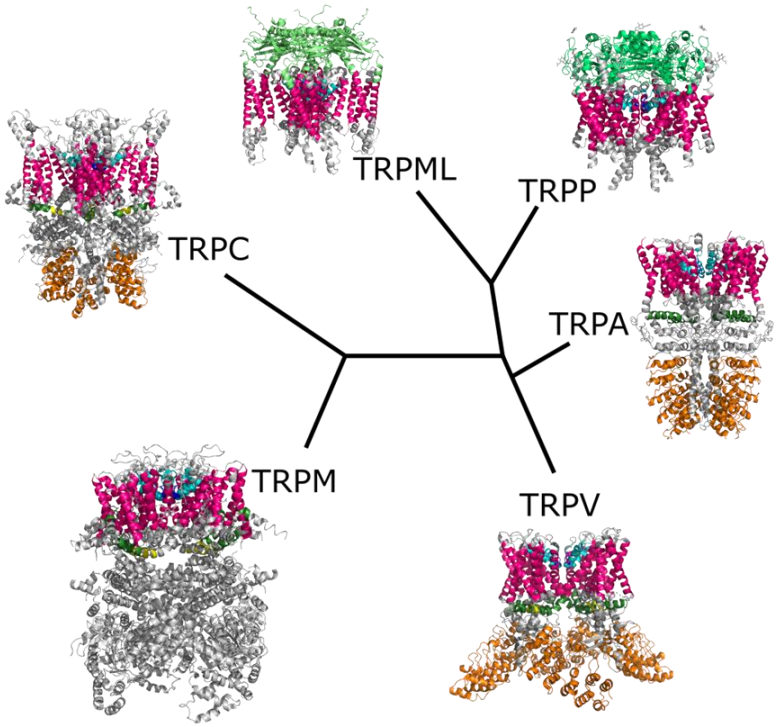

Figure 3: Cladogram of mammalian TRP channel subfamilies and their structures. A representative structure of a member of each subfamily is illustrated: hTRML1 (PDB ID: 5WJ9), hTRPP2 (5K47), hTRPA1 (3J9P), rTRPV1 (3J5P), hTRPM4 (6BQR) and hTRPC3 (6CUD). Specific domains are indicated with the following color code: Pink = transmembrane domains (S1-S6), light blue = pore region, dark blue = selectivity filter, orange = ankyrin repeat domain, dark green = TRP domain, yellow = TRP box, lime = S1-S2 extracellular domain (TRPML and TRPP).

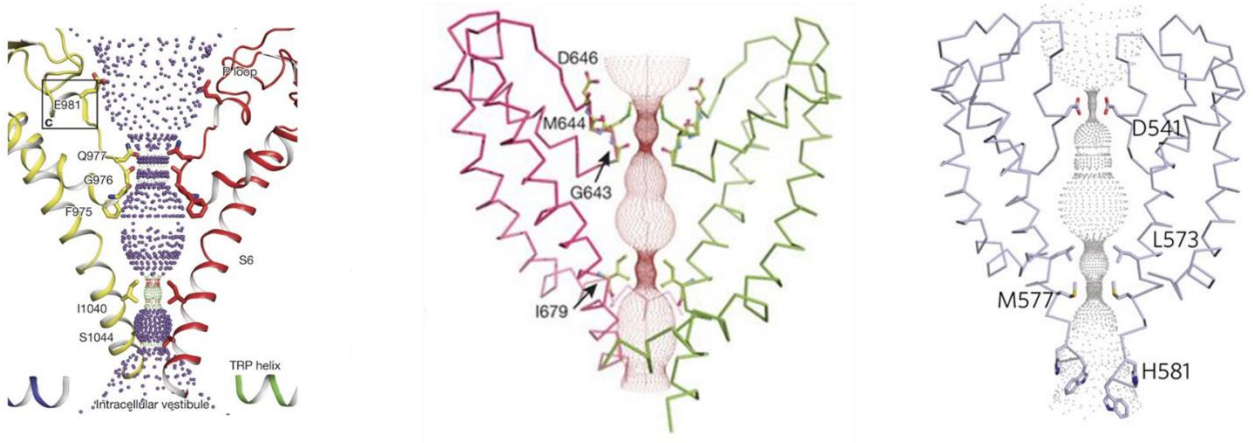

Figure 4: Structure of TRP channel pores. Comparison of the pore domains of TRPM4 (left, Ca^{2+}-impermeable), TRPV1 (middle, Ca^{2+}-permeable, non-selective) and TRPV6 (right, Ca^{2+}selective).

Structures are adapted from Winkler et al, 2017 (TRPM4), Liao et al, 2013 (TRPV1-apo state) and Hughes et al, 2018 (TRPV6). See text for more details.

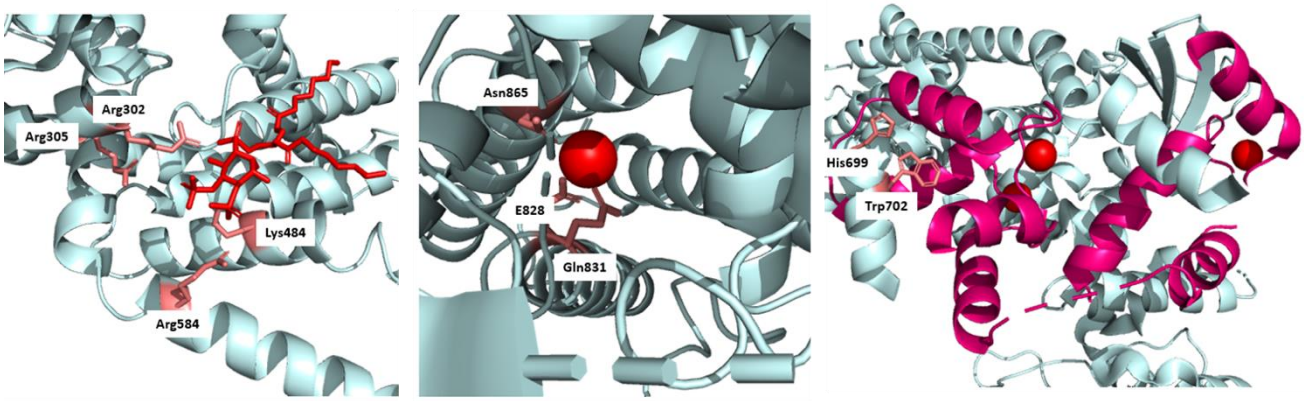

Figure 5: Structural elements underlying Ca^{2+}-dependent regulation of TRP channels. Left: Interaction between PIP_2 and the PIP_2 binding pocket in TRPV5, which is formed by residues from the N terminus (Arg302, Arg305), the S4-S5 linker (Lys484) and the S6-helix (Arg584). PIP_2 is shown in red, interacting amino acids in salmon. Center: a Ca^{2+} ion (red) interacting with TRPM4 via residues Glu828, Gln831 (from S2) and Asn865 and Asp868 (from S3). Right: Ca^{2+} ions bound to calmodulin (red), interacting with the C terminus of TRPV5 via an interaction with His699, Trp702 and Thr709 (salmon).

Table 1: activation and regulation mechanisms of TRP channels

	Representative Ligand	$[Calcium]_I$	T°	Voltage dependence
TRPA1	AITC	+ : direct (low Ca^{2+}) - : direct/CaM (high Ca^{2+})	❄ 🔥	⚡
TRPC1				
TRPC2	DAG	- :		
TRPC3	DAG	- : CaM		
TRPC4	Gd^{3+}	- : CaM		
TRPC5	Gd^{3+}	+: Ca^{2+}	❄	⚡
TRPC6	DAG			
TRPC7	DAG	- : CaM		
TRPM1	PS			
TRPM2	2'-deoxy-ADPR	+ : CaM, direct		
TRPM3	PS, CIM0216	- : PIP_2 depletion	🔥	⚡
TRPM4	Decavanadate	+ : direct - : PIP_2 depletion	🔥	⚡
TRPM5	Ca^{2+}	+ : direct - : PIP_2 depletion	🔥	⚡
TRPM6		- : PIP_2 depletion		
TRPM7	Naltriben	- : PIP_2 depletion		
TRPM8	Menthol	- : PIP_2 depletion	❄	⚡
TRPML1	$PI(3,5)P_2$	- : direct Ca^{2+} block		
TRPML2	SF-11, SN-1			
TRPML3	SF-21/41/81			
TRPP1-PKD2		+ : direct		⚡
TRPP2-PKD2-L1				
TRPP3-PKD2-L2				
TRPV1	Capsaicin	- : CaM, PIP_2 depletion	🔥	⚡
TRPV2	THC	- : PIP_2 depletion	🔥	
TRPV3	2-APB	+ : CaM + direct	🔥	⚡
TRPV4	GSK-1016790A	+ : CaM - : desensitization (?)	🔥	
TRPV5		- : CaM, Calbindin-D28K, PIP_2 depletion		
TRPV6		- : CaM, PIP_2 depletion		

❄ :Cold temperatures; 🔥 :Warm temperatures, ⚡ :Voltage-gated

<u>Abbreviations</u>

2-APB: 2-Aminoethoxydiphenyl borate
AICT: Allyl isothiocyanate
CaM: Calmodulin
DAG: Diacylglycerol
PIP_2: Phosphatidylinositol bisphosphate
PS: Pregnenolone sulfate
SF, SN: Sulfonamides
THC: Tetrahydrocannabinol

Table 2: overview of structures of integral TRP channel proteins

	Species	Method	Resolution	Condition & State	Author	PDB
TRPA1	Human	Cryo-EM	4Å	Agonist AITC Antagonist HC-030031 +/- A-967079	(Paulsen et al. 2015)	3J9P
TRPC1						
TRPC2						
TRPC3	Human	Cryo-EM Lipid nanodisc	4.4 Å	Lipid-activator OAG pore in closed state	(Tang et al. 2018)	5ZBG
	Human	Cryo-EM	3.3 Å	Lipid-ocupied. Closed state	(Fan et al. 2018)	6CUD
	Human	Cryo-EM	5.8 Å	In detergent (GDN)	(Sierra-Valdez et al. 2018)	6DJS/R
TRPC4	Zebrafish	Cryo-EM	3.6 Å	Apo state - closed	(Vinayagam et al. 2018)	6G1K
	Mouse	Cryo-EM	3.3 Å	Apo state – closed/inactivated state	(Duan et al. 2018a)	5Z96
TRPC5						
TRPC6	Human	Cryo-EM Lipid nanodisc	3.8 Å	Complex with inhibitor BTDM - closed	(Tang et al. 2018)	5YX9
TRPC7						
TRPM1						
TRPM2	*Nematostella vectensis*	Cryo-EM	3 Å	Ca^{2+}-bound closed state	(Zhang et al. 2018b)	6CO7
	Zebrafish	Cryo-EM	3.8 Å 3.3 Å	Apo state (closed) ADPR/Ca^{2+}- bound state (active)	(Huang et al. 2018)	6DRK 6DRJ
	Human	Cryo-EM	3.6 Å	Apo State ADPR-bound ADPR/Ca^{2+}-bound	(Wang et al. 2018)	6MIX 6MIZ 6MJ2
TRPM3						
TRPM4	Human	Cryo-EM Lipid nanodisc	3 Å	Ca^{2+}-free state Ca^{2+}-bound state	(Autzen et al. 2018)	6BQR 6BQV
	Human	Cryo-EM	3.7 Å	closed, Na^{+}-bound, apo state	(Duan et al. 2018c)	6BWI
	Mouse	Cryo-EM	3 Å	Without ATP ATP-bound	(Guo et al. 2017)	6BCJ 6BCL 6BCO 6BCQ
	Human	Cryo-EM	3.8 Å	Bound to Ca^{2+} (agonist) and to decavanadate (DVT)	(Winkler et al. 2017)	5WP6
TRPM5						
TRPM6						
TRPM7	Mouse	Cryo-EM	3.28 Å 3.7 Å 4.1 Å	With EDTA Mg^{2+}-bound Mg^{2+}-unbound (Divalent free)	(Duan et al. 2018b)	5ZX5 6BWD 6BWF
TRPM8	*Ficedula albicollis*	Cryo-EM	4.1 Å	Non-conducting state	(Yin et al. 2018)	6BPQ
TRPM L1	Mouse	Cryo-EM in - nanodisc - Amphipols	 5.4 Å 5.8 Å 7.4 Å 7.7 Å	 Closed state State1 (closed) State2 (wide upper gate) State3 (wide lower gate)	(Zhang et al. 2017)	 5YE5 5YE2 5YDZ 5YE1
	Mouse	Cryo-EM in lipid nanodisc	3.59 Å 3.64 Å 3.75 Å	Open state Closed 1 Closed 2	(Chen et al. 2017)	5WPV 5WPQ 5WPT
	Human	Cryo-EM	3.72 Å 3.49 Å	Apo-structure (closed) Agonist bound (open)	(Schmiege et al. 2017)	5WJ5 5WJ9
	Human	Cryo-EM	3.6 Å	PI(3,5)P_2-bound PI(4,5)P_2-bound PI(3,5)P_2/ML-SA1-bound	(Fine et al. 2018)	6E7P 6E7Y 6E7Z
TRPM L2						
TRPM L3	*Callithrix jacchus*	Cryo-EM	2.9 Å	Open state	(Hirschi et al. 2017)	5W3S
	Human	Cryo-EM	4.06 Å 3.62 Å 4.65 Å	Apo channel TRPML3/ML-SA1 complex At pH 4.8	(Zhou et al. 2017)	6AYE 6AYF 6AYG
TRPP1 – PKD2	Human	Cryo-EM in lipid nanodisc	3.0 Å	Closed/non-conductive state	(Shen et al. 2016)	5T4D
	Human	Cryo-EM	3.5 Å	PKD2-F604P mutant	(Zheng et al. 2018)	6D1W

	Human	Cryo-EM	4.2 Å	Both gates closed	(Grieben et al. 2017)	5K47
TRPP2 – PKD2-L1	Human	Cryo-EM	4.3 Å	In complex with cations & lipids – different activation states	(Wilkes et al. 2017)	5MKF 5MKE
	Human	Cryo-EM	3.3 Å		(Hulse et al. 2018)	6DU8
	mouse	Cryo-EM	3.38 Å	Open state	(Su et al. 2018b)	5Z1W
TRPP3 – PKD2-L2						
PKD1 + TRPP1	Human	Cryo-EM	3.6 Å	PKD1/PKD2 complex assembled in a 1:3 ratio	(Su et al. 2018a)	6A70
TRPV1	Rat	Cryo-EM	3.28 Å	Apo state - closed	(Liao et al. 2013)	3J5P (3J9J)
	Rat	Cryo-EM	3.8 Å 4.2 Å	Resiniferatoxin and Capsaicin (activated) Capsazepin (fully open state)	(Cao et al. 2013)	3J5Q, 3J5R
	Rat	Cryo-EM in lipid nanodisc	3.28 Å 3.43 Å 2.95 Å	In complex with Capsazepine In complex with DkTx and RTX	(Gao et al. 2016)	5IRZ 5IS0 5IRX
TRPV2	rabbit	Cryo-EM	4 Å	Nonconductive, desensitized state	(Zubcevic et al. 2016)	5AN8
	Rat	Cryo-EM	~5 Å	Apo state – constitutive activity	(Huynh et al. 2016)	5HI9
	Rabbit	Cryo-EM	3.5 Å	Resiniferatoxin (RTx) and/or Ca^{2+}-bound – open state	(Zubcevic et al. 2018b)	6BWM, 6BWJ
	Rat	Cryo-EM	3,6 Å 4 Å	In partially closed state Open state (resolved pore turret domain)	(Dosey et al. 2018)	6BO5 6BO4
TRPV3	Mouse	Cryo-EM	4.3 Å 4 Å	closed apo Agonist (2-APB)-bound open states (+mutant)	(Singh et al. 2018a)	6DVW 6DVY/Z
	Human	Cryo-EM	3.4 Å 3.2 Å <3.5 Å	Apo state Sensitized conformation In the presence of 2-APB	(Zubcevic et al. 2018a)	6MHO 6MHS 6MHV/W/X
TRPV4	*Xenopus laevis*	Cryo-EM + Crystal structure	3.8 Å	Apo state – closed state In the presence of cesium, Barium, gadolinium	(Deng et al. 2018)	6BBJ 6C8F, 6C8G, 6C8H
TRPV5	Rabbit	Cryo-EM	3,5-4 Å	In complex with its inhibitor econazole – closed state	(Hughes et al. 2018a)	6B5V
	Rabbit	Cryo-EM		Lipid-bound in detergent $PI(4,5)P_2$-bound in nanodisc CaM-bound in detergent	(Hughes et al. 2018b)	6DMR 6DMU 6DMW
TRPV6	Rat	Crystal structure	3.25 Å	TRPV6 In the presence of Ca^{2+} (open state) Barium Gadolinium	(Saotome et al. 2016)	5IWK 5IWP 5IWR 5IWT
	Human Rat	Cryo-EM	3.6 Å 4.0 Å	In nanodiscs In amphipols TRPV6-R470E in amphipols TRPV6 in nanodisc	(McGoldrick et al. 2018)	6BO8 6BO9 6BOA 6BOB
	Rat	Crystal	3.45 Å	In complex with 2-APB In complex with 2-APB-Br Y466A Y466A + in complex with 2-APB Y467A Y467A + in complex with 2-APB	(Singh et al. 2018c)	6DO7 6D7V 6D7P 6D7Q/X 6D7S 6D7T
	Human Rat	Cryo-EM	3.9 Å 3.6 Å	TRPV6 in complex with Calmodulin TRPV6 in complex with Calmodulin	(Singh et al. 2018b)	6E2F 6E2G